

RESEARCH ARTICLE

Characterization of [^{11}C]PXT012253 as a PET Radioligand for mGlu $_4$ Allosteric Modulators in Nonhuman Primates

Akihiro Takano,¹ Sangram Nag,¹ Zhisheng Jia,¹ Mahabuba Jahan,¹ Anton Forsberg,¹ Ryosuke Arakawa,¹ Per Grybäck,^{2,3} Guillaume Duvey,⁴ Christer Halldin,¹ Delphine Charvin⁴

¹Department of Clinical Neuroscience, Center for Psychiatry Research, Karolinska Institutet and Stockholm County Council, Stockholm, Sweden

²Department of Medical Radiation Physics and Nuclear Medicine, Karolinska University Hospital, Solna, Sweden

³Department of Molecular Medicine and Surgery, Karolinska Institute, Stockholm, Sweden

⁴Prexton Therapeutics, 14 Chemin des Aulx, 1228, Plan-les-Ouates, Geneva, Switzerland

Abstract

Purpose: Modulation of presynaptic metabotropic glutamate receptor 4 (mGlu $_4$) by an allosteric ligand has been proposed as a promising therapeutic target in Parkinson's disease and levodopa-induced dyskinesia. A positron emission tomography (PET) ligand for an allosteric site of mGlu $_4$ may provide evidence that a clinical drug candidate reaches and binds the target. A carbon-11-labeled PET radioligand binding an allosteric site of mGlu $_4$, [^{11}C]PXT012253, has been recently developed. Here, we describe the detailed characterization of this novel radiolabeled mGlu $_4$ ligand in nonhuman primates.

Procedures: [^{11}C]PXT012253 binding in the brain of cynomolgus monkeys, under the baseline and blocking conditions with the structurally different mGlu $_4$ allosteric ligand PXT002331, currently in clinical trials for Parkinson's disease, was quantified with compartment and graphical modeling approaches using a radiometabolite-corrected plasma input function. Whole-body biodistribution of [^{11}C]PXT012253 was then assessed using PET/x-ray computed tomography to estimate the human effective doses of [^{11}C]PXT012253 for further clinical studies.

Results: [^{11}C]PXT012253 displayed binding in mGlu $_4$ -expressing regions in the brain of cynomolgus monkeys. Brain regional time-activity curves of [^{11}C]PXT012253 were well described in the two-tissue compartment model (2TC). Total distribution volume was stably estimated using Logan plot and multilinear analysis (MA1) although 2TC showed unstable values in some cases. Competition with PXT002331 showed high specific binding in the total distribution volume. Whole-body PET showed high accumulation of [^{11}C]PXT012253 in the liver, kidney, heart, and brain in the initial phase. The radioligand was excreted through both the gastrointestinal and the urinary tracts. Effective dose of [^{11}C]PXT012253 was estimated to be 0.0042 mSv/MBq.

Electronic supplementary material The online version of this article (<https://doi.org/10.1007/s11307-018-1257-0>) contains supplementary material, which is available to authorized users.

Correspondence to: Christer Halldin; e-mail: Christer.Halldin@ki.se, Delphine Charvin; e-mail: Delphine.Charvin@prextontherapeutics.com

Conclusions: [¹¹C]PXT012253 was shown to be a promising PET radioligand for mGlu₄ allosteric modulators in the monkey brain. MA1 would be the choice of quantitative method. Further development of [¹¹C]PXT012253 in human subjects is warranted.

Key words: Metabotropic glutamate receptor 4, Positron emission tomography, Dosimetry, Brain, Primate, Foliglurax, Radiotracer, Glutamate, Allosteric

Introduction

Metabotropic glutamate (mGlu) receptors are one of the two major classes of glutamate receptors; they have eight subtypes (mGlu₁ to mGlu₈). Development of positron emission tomography (PET) radioligands for mGlu₁ and mGlu₅ has been successful, and the utility of radioligands such as [¹⁸F]FIMX for mGlu₁ and [¹⁸F]FPEB, [¹⁸F]SP203, and [¹¹C]ABP688 for mGlu₅ has been demonstrated in clinical trials [1–6].

Because mGlu₄ activation was reported to have potential benefits in treating neurological diseases such as Parkinson's disease (PD) and levodopa-induced dyskinesia (LID) [7, 8], the research for mGlu₄ positive allosteric modulators (PAM) has been initiated more than a decade ago [9] and made a big leap this year with the first mGlu₄ PAM entering in the clinic (PXT002331) [10]. Consequently, the need for PET radioligand targeting mGlu₄ has increased for several reasons: (i) to further characterize the target in the human brain, visualizing and quantifying mGlu₄ binding in living human subjects, because the comparison of mGlu₄ binding between the patients with neurological diseases and healthy controls may be useful for the understanding of the pathophysiology and treatment of the diseases, and (ii) to support clinical development of mGlu₄ allosteric modulators.

Recently, [¹¹C]PXT012253 (formerly [¹¹C]11 and [¹¹C]KALB012), which has high affinity to mGlu₄ (3.4 nM), has been successfully developed and evaluated in rodents [11, 12]. In this study, in order to characterize [¹¹C]PXT012253 for further application in clinical studies, we used nonhuman primates (NHP) to perform the quantitative analysis of *in vivo* brain kinetics of [¹¹C]PXT012253 and biodistribution in the whole body for dosimetry calculation by PET measurements.

Materials and Methods

Subjects

Three male cynomolgus monkeys (NHP1–NHP3) (body weight 6.4–8.3 kg) were used in the brain PET study and two female cynomolgus monkeys (NHP4 and NHP5) (body weight 5.6 and 6.3 kg) were used in the whole-body PET study. The NHPs were housed in the Astrid Fagraeus Laboratory (AFL) of the Swedish Institute for Infectious Disease Control, Solna, Sweden. The study was approved by the Animal Ethics Committee of the Swedish Animal Welfare

Agency and was performed according to “Guidelines for planning, conducting and documenting experimental research” (Dnr 4820/06-600) of Karolinska Institutet.

Radioligand Synthesis of [¹¹C]PXT012253

[¹¹C]Methane ([¹¹C]CH₄) was produced in-target *via* the ¹⁴N(p,α)¹¹C reaction on nitrogen mixed with 10 % of hydrogen, with 16.4 MeV protons using a GEMS PET trace cyclotron (GE, Uppsala, Sweden). Typically, the target gas was irradiated for 15–20 min with a beam current of 35 μA. ¹¹C-Labeled methyl iodide, [¹¹C]CH₃I, was produced following the previously published method [13]. In short, the produced [¹¹C]CH₄ was released from the target and collected in a Porapak Q trap cooled in liquid nitrogen. After collection, the [¹¹C]CH₄ was released from the trap by heating with pressurized air, and subsequently [¹¹C]CH₄ was mixed with vapors from iodine crystals at 60 °C followed by a radical reaction at 720 °C. The formed [¹¹C]CH₃I was collected in a Porapak Q trap at room temperature and the unreacted [¹¹C]CH₄ was recirculated for 3 min. [¹¹C]CH₃I was released from the Porapak Q trap by heating the trap using a custom-made oven at 180 °C. [¹¹C]CH₃OTf was produced by online transfer of [¹¹C]CH₃I through a glass column packed with silver triflate at 165 °C.

[¹¹C]PXT012253 was obtained by trapping [¹¹C]CH₃OTf at room temperature in a reaction vessel containing the desmethyl thiophenol precursor PXT012252 (0.5–1.0 mg, 1.9–3.8 μmol) and potassium carbonate (K₂CO₃) (10–13 mg, 178–232 μmol) in acetone (300 μl) (Fig. 1). After end of trapping, the reaction mixture was diluted with sterile water (500 μl) before injecting to the built-in high-performance liquid chromatography (HPLC) system for the purification of the desired radiolabeled product. The HPLC system consisted of a semi-preparative reverse phase (RP) ACE column (C18, 10 × 250 mm, 5 μm particle size) and a Merck Hitachi UV detector (λ = 254 nm) (VWR, International, Stockholm, Sweden) in series with a GM-tube (Carroll-Ramsey, Berkley, CA, USA) used for radioactivity detection. The radioactive fraction corresponding to pure [¹¹C]PXT012253 was collected from HPLC and evaporated to dryness. The final purified [¹¹C]PXT012253 was formulated in 6 ml phosphate-buffered saline (PBS) (pH 7.4) and found to be stable after 1 h. The formulated product was then sterile filtered through a Millipore Millex® GV filter unit (0.22 μm) for further use *in vivo*.

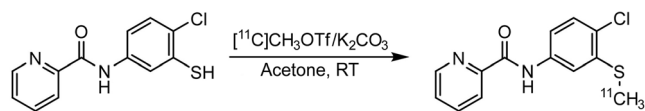


Fig. 1. The scheme of radiosynthesis of [¹¹C]PXT012253.

NHP Brain PET

PET System PET measurements were conducted using a high-resolution research tomograph (HRRT) (Siemens Molecular Imaging). List mode data were reconstructed using the ordinary Poisson-3D-ordered subset expectation maximization (OP-3D-OSEM) algorithm, with 10 iterations and 16 subsets including modeling of the point spread function (PSF) [14]. The corresponding in-plane resolution with OP-3D-OSEM PSF was 1.5 mm full width at half-maximum (FWHM) in the center of the field of view (FOV) and 2.4 mm at 10-cm off-center directions.

PET Measurements Anesthesia was induced by intramuscular injection of ketamine hydrochloride (approximately 10 mg/kg) at AFL and maintained by the administration of a mixture of sevoflurane (0–8.0 %), oxygen, and medical air with endotracheal intubation in the KI PET center. The NHP head was immobilized with a fixation device. Body temperature was maintained by a Bair Hugger model 505 (Arizant Healthcare, MN) and monitored by an esophageal thermometer. ECG, heart rate, blood pressure, respiratory rate, and oxygen saturation were continuously monitored throughout the experiments. Fluid balance was maintained by continuous infusion of saline.

A transmission scan of 6 min using a single Cs-137 source was performed before the radioligand injection. List mode data were acquired continuously for 95 min immediately after i.v. injection of the radioligand. Images were reconstructed with a series of 38 frames (10 s × 9, 15 s × 2, 20 s × 3, 30 s × 4, 1 min × 4, 3 min × 4 and 6 min × 12).

PXT002331 Administration After the baseline PET measurement, 2 mg/kg of PXT002331 was administered intravenously with bolus infusion in one NHP (NHP2). Duration of infusion was 2 min at 5 min before PET scanning. PXT002331 was formulated by dissolving in DMSO (5 %), kolliphor EL (15 %), and PBS (80 %). The pH of final dose was approximately 4.5–5.0.

Arterial Blood Sampling Automated blood sampling system (ABSS) was used to measure the continuous radioactivity for the first 3 min after the radioligand injection. Blood sampling was performed manually for the measurement of metabolism and radioactivity at 4, 15, 30, 60, and 90 min after the injection.

Metabolite Analysis The amount of unchanged [¹¹C]PXT012253 and its radioactive metabolites in NHP plasma were measured by a reversed-phase radio-HPLC method. The plasma was separated from blood by centrifuging at 2000×g for 2 min. The obtained plasma was mixed with 1.4 times volume of acetonitrile and centrifuged at 2000×g for 4 min and the extract was injected into an online radio-HPLC system. An Agilent binary pump (Agilent 1200 series) coupled to a manual injection valve (7725i, Rheodyne), 1–3.0 ml loop, and a radiation detector (Oyokoken, S-2493Z) housed in a shield of 50-mm-thick lead was used for metabolite measurements. Data collection and control of the LC system was performed using chromatographic software (ChemStation Rev. B.04.03; Agilent). The accumulation time of radiation detector was 10 s. Chromatographic separation was performed with a ACE C18 column (250 mm × 10 mm I.D.), by gradient elution. Acetonitrile (A) and 10 mM ammonium formate (B) were used as the mobile phase at 5.0 ml/min, according to the following program: 0–3.0 min, (A/B) 60:40 → 80:20 v/v; 3.0–5.0 min, (A/B) 80:20 → 90:10 v/v; 5.0–10.0 min, (A/B) 90:10 v/v. Peaks for radioactive compounds eluting from the column were integrated, and their areas were expressed as a percentage of the sum of the areas of all detected radioactive compounds (decay-corrected to the time of injection on the HPLC).

Protein Binding To measure the protein binding in plasma, a blood sample was taken 3 min before injection of [¹¹C]PXT012253. The free fraction (f_p) of [¹¹C]PXT012253 in plasma was estimated using an ultrafiltration method. Plasma (300 μl) or phosphate-buffered saline solution (300 μL) as a control was mixed with [¹¹C]PXT012253 (30 μl, ~1 MBq) and incubated at room temperature for 10 min. After the incubation, 200-μl portions of the incubation mixtures were pipetted into ultrafiltration tubes (Centrifree YM-30, molecular weight cutoff, 30,000 Da; Millipore: Billerica, USA) and centrifuged at 1500×g for 15 min. Equal aliquots (20 μl) of the ultrafiltrate (C_{free}) and of the plasma (C_{total}) were counted for their radioactivity with a NaI well-counter. Each determination was performed in duplicate. The free fraction was then calculated as $f_p = C_{free}/C_{total}$, and the results were corrected for the membrane binding measured with the control samples.

Image Analysis The regions of interest (ROIs) were delineated manually on the MRI images of each NHP for the whole brain, caudate, putamen, thalamus, hippocampus, amygdala, anterior cingulate cortex, cerebellum, occipital cortex, parietal cortex, temporal cortex, frontal cortex, and pons. The summed PET images of the whole scan were co-registered to the MRI image of the individual NHP. By applying the co-registration parameters to the dynamic PET data, the time-activity curves (TACs) of brain regions were generated for each PET measurement.

Kinetic Model Analysis As the outcome measure, the total distribution volume (V_T) was calculated with metabolite-corrected plasma radioactivity as the input function. Four models were used for calculation of V_T ; K_1/k_2 by the one-tissue compartment (1TC) model, $(K_1/k_2) \times (k_3/k_4 + 1)$ by two-tissue compartment (2TC) model, Logan graphical analysis [15], and MA1 [16]. The fitness of model curves in 1TC and 2TC were evaluated by the model selection criterion (MSC), which is the modified Akaike Information Criterion (AIC) by normalizing of the magnitude of data points [17]. The identifiability of V_T in Logan plot and MA1 was evaluated by the percentage of the coefficient of variation (%COV). These analyses were performed using the PMOD 3.4 software package (PMOD Group, Zurich, Switzerland).

Blocking Effects by PXT002331 V_T consists of the displaceable and nondisplaceable parts (V_{ND}). The blocking effects by PXT002331 were evaluated using the Lassen plot [18], which can estimate the target occupancy and V_{ND} . V_T values by MA1 were used for this evaluation.

NHP Whole-Body PET

PET System Whole-body PET scans were conducted using a GE Discovery PET/X-ray computed tomography (CT) 710 (GE healthcare, Waukesha, WI, USA). PET images were reconstructed with a 3D ordered subset expectation maximization (OSEM) algorithm with three iterations and 18 subsets, including the time of flight information (VUE Point FX) and the point spread function correction (Sharp IR). 2D Gaussian filter with 5.5 mm cutoff was used.

PET Measurements Anesthesia was induced by intramuscular injection of ketamine hydrochloride (approximately 10 mg/kg) at AFL and maintained by intravenous infusion of ketamine (4 mg/kg/h) and xylazine (0.4 mg/kg/h) with pump. The body of the NHP was immobilized using a vacuum pad. Body temperature was maintained by a Bair Hugger model 505 (Arizant Healthcare, MN) and monitored by an esophageal thermometer. ECG, heart rate, blood pressure, respiratory rate, and oxygen saturation were

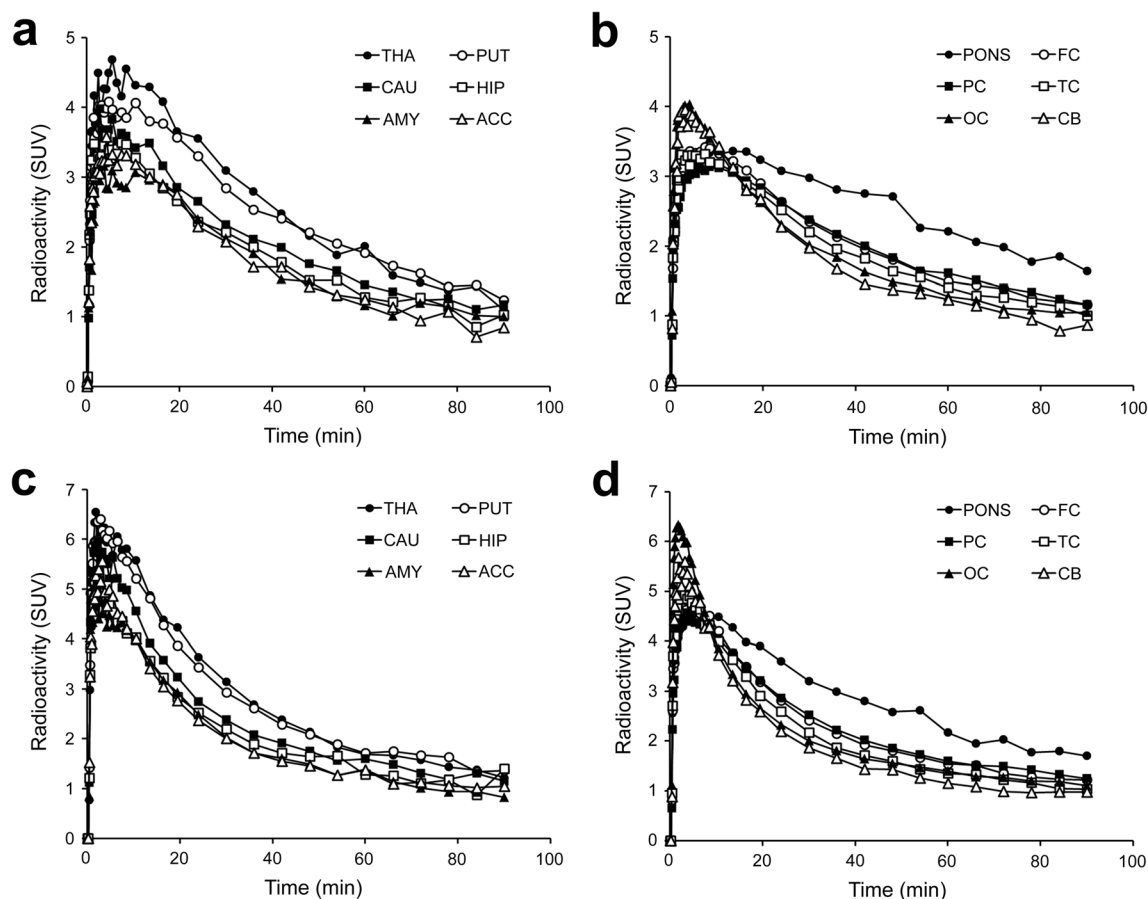


Fig. 2. Regional time-activity curves of one representative NHP at the baseline (a and b), and under the blocking condition with PXT002331 (c and d). THA thalamus, PUT putamen, CAU caudate, HIP hippocampus, AMY amygdala, ACC anterior cingulate cortex, PONS pons, FC frontal cortex, PC parietal cortex, TC temporal cortex, OC occipital cortex, CB cerebellum.

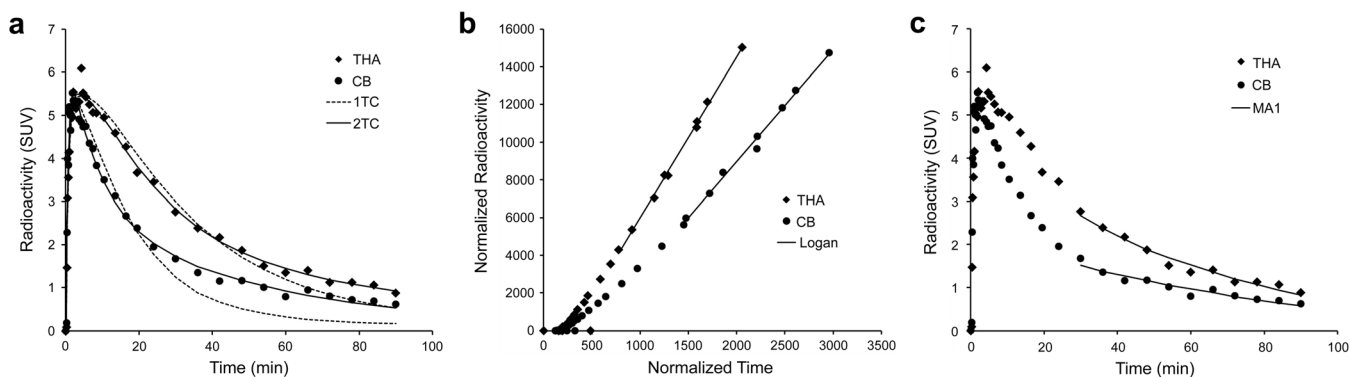


Fig. 3. Model fitting curves of the thalamus and cerebellum in one representative NHP (NHP2) with four models. (a) 1TC and 2TC. (b) Logan plot. (c) MA1. *THA* thalamus, *CB* cerebellum.

continuously monitored throughout the experiments. Fluid balance was maintained by continuous infusion of saline.

One low-dose CT scan was performed before intravenous administration of the radioligand for attenuation correction. Then, four series of PET acquisitions, each covering five axial fields of view (AFOV), were conducted. The four PET series consisted of two 20 s × 5 AFOV scans, three 40 s × 5 AFOV scans, four 80 s × 5 AFOV scans, and six 160 s × 5 AFOV scans, respectively. The time for the bed to return to the original position was approximately 20 s, and the total duration of the whole-body scan was 125 min.

Image Analysis ROIs were drawn on the heart, liver, kidney, spleen, lung, parotid gland, submandibular gland, thyroid, brain, bone marrow (lumbar vertebra), gall bladder, small intestine, and urinary bladder with the help of the 3D-CT images for anatomic landmarks. Radioactivity concentration in each PET scan was decay-corrected to the time of injection. Time-activity curve was expressed as percentage of the injected

dose (%ID) calculated as follows: radioactivity (Bq/cc) × ROI volume (cc)/injected dose (Bq) × 100.

Estimates of the absorbed radiation dose in humans were calculated with the OLINDA/EXM 1.1 (Organ Level Internal Dose Assessment Code) software, using the adult male (70 kg) reference model [19]. The fractional uptake in NHP organs was assumed to be equal to the uptake in human organs.

Results

NHP Brain PET

The injected radioactivity of [¹¹C]PXT012253 (*n* = 4) was 154 ± 8 (mean ± SD) (range 143–161) MBq. The molar radioactivity at the time of injection was 770 ± 792 (139–1924) GBq/μmol, and the injected mass was 0.13 ± 0.13 (0.02–0.32) μg, respectively.

The uptake of whole brain reached peak at 4 min, and it decreased to half in around 40 min on average of three

Table 1. Mean V_T and MSC by 1TC and 2TC

	1TC	MSC	2TC	MSC
CAU	5.8	3.1	6.6	3.6
PUT	6.8	3.3	7.4	3.9
THA	7.7	3.7	7.8	3.9
HIP	4.8	2.7	6.3	3.3
AMY	5.1	2.7	5.4	2.8
ACC	5.0	3.3	6.1	3.6
CB	4.4	3.2	6.2	4.5
OC	4.8	2.9	7.2	5.4
PC	6.0	3.8	7.3	4.3
TC	5.1	3.6	6.3	4.5
FC	5.3	3.7	6.2	4.1
PONS	8.3	3.4	9.1	4.3
Mean		3.3		4.0

V_T and MSC by 2TC with unreliable estimation (%COV > 25 %) in 5/36 excluded. The number of NHPs is three
CAU caudate, *PUT* putamen, *THA* thalamus, *HIP* hippocampus, *AMY* amygdala, *ACC* anterior cingulate cortex, *CB* cerebellum, *OC* occipital cortex, *PC* parietal cortex, *TC* temporal cortex, *FC* frontal cortex

Table 2. Mean V_T and %COV by Logan plot and MA1

	Logan	%COI	MA1	(%COI)
CAU	7.3	2.9	6.9	1.8
PUT	7.9	3.7	7.9	1.6
THA	8.1	1.8	8.0	1.2
HIP	5.7	3.7	5.7	1.5
AMY	5.6	4.5	5.6	1.4
ACC	6.1	4.0	6.0	1.6
CB	5.9	3.0	5.7	1.4
OC	6.7	2.4	6.3	1.9
PC	7.1	1.8	6.8	1.9
TC	6.2	2.3	6.0	1.6
FC	6.5	2.1	6.2	1.7
PONS	8.7	2.3	8.8	2.3
Mean		2.9		1.7

The number of NHPs is three
CAU caudate, *PUT* putamen, *THA* thalamus, *HIP* hippocampus, *AMY* amygdala, *ACC* anterior cingulate cortex, *CB* cerebellum, *OC* occipital cortex, *PC* parietal cortex, *TC* temporal cortex, *FC* frontal cortex

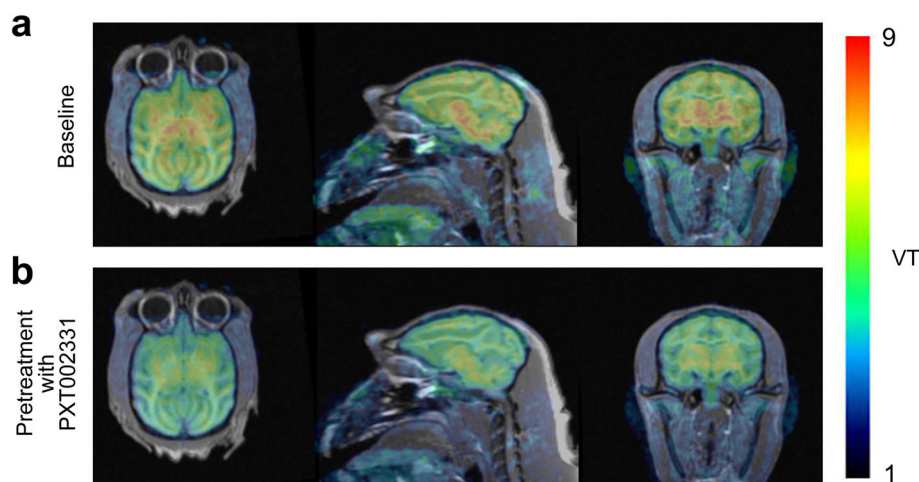


Fig. 4. Parametric images of baseline (a) and pretreatment (b) conditions by Logan plot. Representative results in **a/** vehicle- (baseline) or **b/** PXT002331 (2 mg/kg, iv, pretreatment) -injected macaque. Horizontal (left), sagittal (middle) and coronal (right panel) PET images and corresponding anatomical T1-weighted MRI images.

NHPs. The mean peak of %ID (injected dose) of whole brain was 3.6 %. Regional brain TACs of one representative NHP are shown in Fig. 2a, b at the baseline and in Fig. 2c, d under the blocking condition. The highest uptakes were observed in the thalamus and putamen. The pons showed relatively slow kinetics. TACs of mean three NHPs at the baseline are shown in Suppl. Fig. 1a and b (see Electronic Supplementary Material: ESM).

[¹¹C]PXT012253 was metabolized as 34.8 % at 15 min and 8.7 % at 90 min on average of three NHPs at baseline condition. A typical radio-HPLC chromatogram is shown in

Suppl. Fig. 2 (ESM). The radiometabolites detected were more polar than the parent radioligand. Mean protein binding was 95.4 %.

Regional TACs were well described with 2TC, but not well with 1TC in some cases (Fig. 3a). Both Logan plot and MA1 were well fitted (Fig. 3b, c).

Although the fits of the 2TC model were good, some V_T values could not be reliably estimated (%COV > 25 % in 5/36). Mean V_T values of three NHPs by 1TC and 2TC models after exclusion of outliers are shown in Table 1. Mean MSC of 2TC was higher than that of 1TC (4.0 vs.

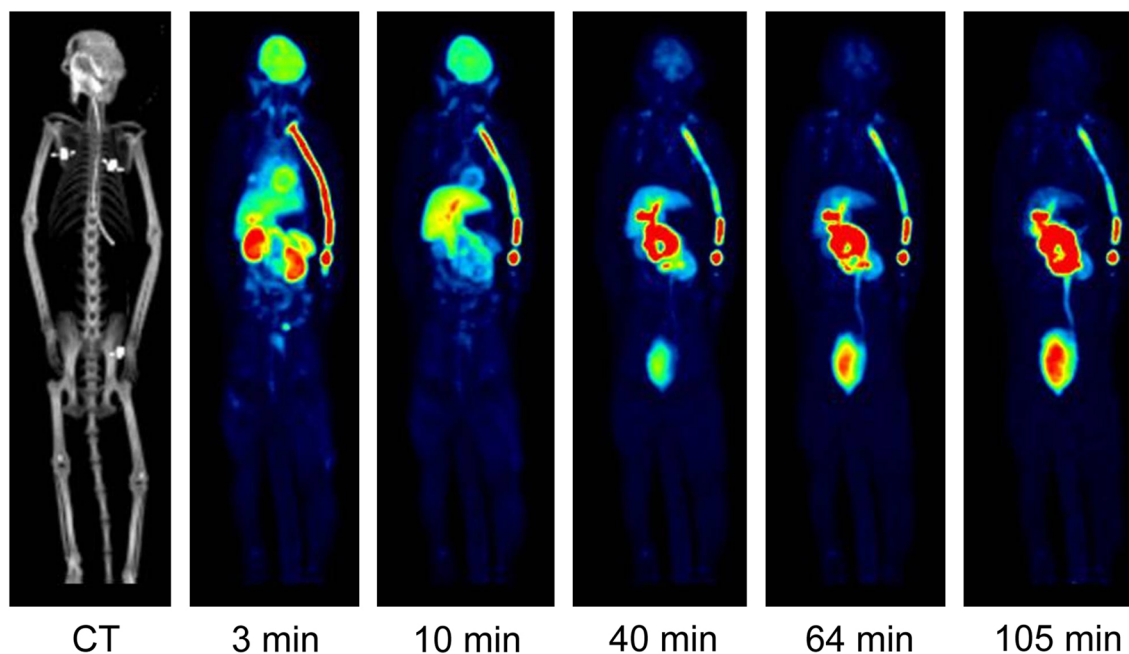


Fig. 5. Whole-body PET images in the time course. PET and CT were maximum intensity projection (MIP) images. The color scales were arbitrary among different time points. Each image at each time point shows the relative accumulation in the whole body.

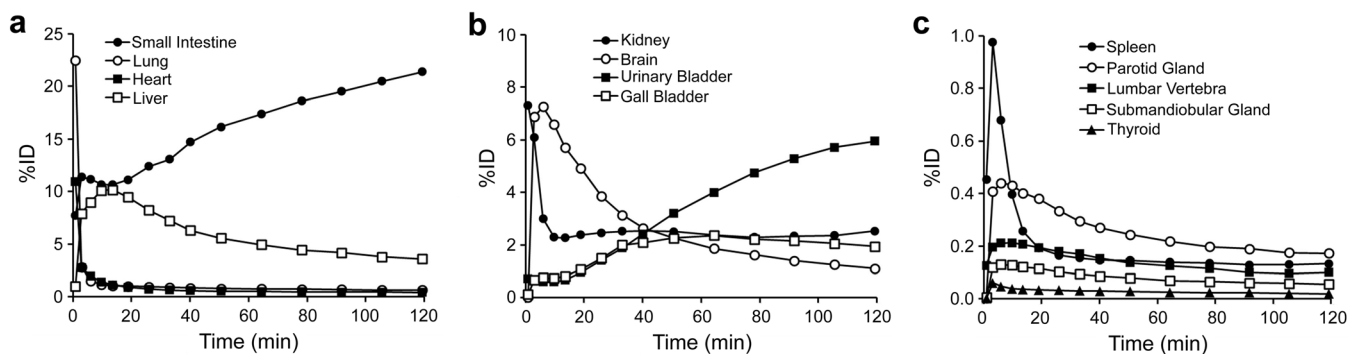


Fig. 6 Time-activity curves of organ uptake. %ID percentage of injected radioactivity dose. **a** High uptake organs. **b** Intermediate uptake organs. **c** Low uptake organs.

3.3), indicating better fitting with 2TC. Mean V_T values by Logan plot and MA1 are shown in Table 2. Mean %COV of MA1 was lower than that of Logan plot (1.7 vs. 2.9 %), indicating well identifiability in MA1.

Parametric images by Logan plot of one NHP, which had two measurements, are shown in Fig. 4. V_T decreased after intravenous administration of 2 mg/kg of PXT002331. Lassen plot using V_T s by MA1 with 2 mg/kg of PXT002331 is shown in Suppl. Fig. 3 (ESM). The target occupancy was 36 %, and V_{ND} was 1.7. There was no clear change of parent fraction (36.5 and 38.2 % at 15 min, 9.3 and 10.2 % at 90 min) and protein binding (93.4 and 94.9 %) before and after drug administration of PXT002331, respectively.

NHP Whole-Body PET

The injected radioactivity of [¹¹C]PXT012253 ($n=2$) was 149 and 201 MBq. The molar radioactivity at the time of injection was 586 and 1298 GBq/ μ mol, and the injected mass was 0.07 and 0.04 μ g, respectively.

Whole-body images over time of one representative NHP are shown in Fig. 5. High uptakes were shown in the small intestine, liver, and brain. Time-activity curves of organ uptake in the unit of %ID are shown in Fig. 6a–c. The numbers of disintegrations are shown in Table 3, and the human radiation dose estimates are shown in Table 4. Human radiation dose estimates indicated that most organs

Table 3. The numbers of disintegrations in the source organs

Source organ	NHP4	NHP5	Mean
Brain	2.20×10^{-2}	2.40×10^{-2}	2.30×10^{-2}
Gallbladder contents	6.30×10^{-3}	5.20×10^{-3}	5.75×10^{-3}
Small intestine	6.20×10^{-2}	7.00×10^{-2}	6.60×10^{-2}
Heart wall	5.90×10^{-3}	4.40×10^{-3}	5.15×10^{-3}
Kidneys	1.56×10^{-2}	5.60×10^{-2}	1.06×10^{-2}
Liver	3.50×10^{-2}	4.60×10^{-2}	4.05×10^{-2}
Lungs	6.80×10^{-3}	6.30×10^{-3}	6.55×10^{-3}
Spleen	1.80×10^{-3}	7.30×10^{-4}	1.27×10^{-3}
Urinary bladder	1.20×10^{-2}	2.70×10^{-2}	1.95×10^{-2}
Remainder	3.20×10^{-1}	3.00×10^{-1}	3.10×10^{-1}

Unit: MBq-hour/MBq administered

appear to receive around 0.001–0.01 mSv/MBq. The small intestine appeared to receive the highest dose, around 0.022 mSv/MBq. The mean effective dose of two NHPs was 0.0042 mSv/MBq.

Discussions

mGlu₄ is an emerging target for drug development of neurological diseases such as Parkinson's disease and levodopa-induced dyskinesia [7–10]. The target occupancy in the living brain might be helpful to build PK/PD relationships of potential drug candidates and evaluate the optimal doses to be used in patients, and also to study disease mechanisms. With [¹¹C]PXT012253, *in vivo*

Table 4. Radiation dose estimates for human (adult male model).

Target organ	NHP4	NHP5	Mean
Adrenals	3.01×10^{-3}	2.80×10^{-3}	2.91×10^{-3}
Brain	5.36×10^{-3}	5.79×10^{-3}	5.58×10^{-3}
Breasts	1.85×10^{-3}	1.75×10^{-3}	1.80×10^{-3}
Gallbladder wall	1.81×10^{-2}	1.57×10^{-2}	1.69×10^{-2}
LLI wall	3.39×10^{-3}	3.57×10^{-3}	3.48×10^{-3}
Small intestine	2.08×10^{-2}	2.31×10^{-2}	2.20×10^{-2}
Stomach wall	2.83×10^{-3}	2.69×10^{-3}	2.76×10^{-3}
ULI wall	4.79×10^{-3}	4.98×10^{-3}	4.89×10^{-3}
Heart wall	6.14×10^{-3}	4.89×10^{-3}	5.52×10^{-3}
Kidneys	1.54×10^{-2}	6.60×10^{-3}	1.10×10^{-2}
Liver	7.02×10^{-3}	8.74×10^{-3}	7.88×10^{-3}
Lungs	2.83×10^{-3}	2.68×10^{-3}	2.76×10^{-3}
Muscle	2.30×10^{-3}	2.25×10^{-3}	2.28×10^{-3}
Ovaries	3.93×10^{-3}	4.15×10^{-3}	4.04×10^{-3}
Pancreas	3.17×10^{-3}	2.97×10^{-3}	3.07×10^{-3}
Red marrow	2.32×10^{-3}	2.26×10^{-3}	2.29×10^{-3}
Osteogenic cells	3.18×10^{-3}	3.04×10^{-3}	3.11×10^{-3}
Skin	1.78×10^{-3}	1.70×10^{-3}	1.74×10^{-3}
Spleen	4.10×10^{-3}	2.34×10^{-3}	3.22×10^{-3}
Testes	2.11×10^{-3}	2.14×10^{-3}	2.13×10^{-3}
Thymus	2.20×10^{-3}	2.06×10^{-3}	2.13×10^{-3}
Thyroid	2.11×10^{-3}	2.00×10^{-3}	2.06×10^{-3}
Urinary bladder wall	1.05×10^{-2}	2.05×10^{-2}	1.55×10^{-2}
Uterus	3.96×10^{-3}	4.42×10^{-3}	4.19×10^{-3}
Total body	2.81×10^{-3}	2.79×10^{-3}	2.80×10^{-3}
Effective dose	3.78×10^{-3}	4.53×10^{-3}	4.16×10^{-3}

Unit: mSv/MBq

imaging of mGlu₄ would be boosted to speed up the research of mGlu₄ allosteric therapies.

In the present study, by performing PET measurements of [¹¹C]PXT012253 in the brain and whole body in NHP, we characterized the brain kinetics and estimated the radiation dosimetry of this novel radioligand.

At baseline condition, the brain uptake of [¹¹C]PXT012253 was 3.6 %ID at the peak and decreased rapidly, which is a suitable kinetic for estimation of PET radioligand in the brain. The regional distribution showed the highest binding in the thalamus and putamen, and the lowest in the cortexes, which is in accordance with previously reported brain expression of mGlu₄ in humans [20]. This pattern was similar to that reported previously in rat brain with the same PET ligand [11] or in NHP brain with another F-18-labeled PET radioligand for mGlu₄ [21]. Thus, the regional distribution of [¹¹C]PXT012253 in NHP brain is considered to reflect the distribution of mGlu₄ receptors although direct comparison could not be made between B_{\max} data and PET data due to lack of B_{\max} of mGlu₄ in NHP brain.

In the compartment model analysis, the 2TC model was visually better fitted to the brain TACs of [¹¹C]PXT012253 than 1TC in some regions. It was confirmed by higher MSC in 2TC than 1TC. However, V_T values could not be reliably estimated by 2TC in some cases. In the linear graphical analysis, both Logan plot and MA1 were well fitted and V_T 's were well correlated with those by 2TC ($R=0.9$ and 0.9 , respectively). As MA1 showed slightly better identifiability than Logan plot with lower %COV, MA1 would be the choice of quantitative method for [¹¹C]PXT012253.

There was a large variability of molar activity of [¹¹C]PXT012253 in this study. When the injected mass was plotted against V_T estimated by MA1, there was no clear indication of the mass effect as shown in Suppl. Fig. 4 (ESM). Therefore, we think that, although it is not optimal to have a large variability of molar activity, it did not affect the results in this study.

The V_T 's decreased after pretreatment of PXT002331 in all regions. It confirms that the expression of mGlu₄ is widespread in the brain [22], and there is no suitable reference region in the primate brain, including the cerebellum for [¹¹C]PXT012253. The Lassen plot described well the target occupancy measured by [¹¹C]PXT012253, although only one dose was tested in the present study. The target occupancy was estimated to be 36.1 %, which was higher than preliminary test-retest variability (15–20 %) of baseline V_T from two NHPs (unpublished data). Estimated V_{ND} by Lassen plot was 1.7, which indicated high amount (around 70–80 % of V_T) of specific binding of [¹¹C]PXT012253. Lassen plot evaluation is based on the assumption that the non-specific binding (V_{ND}) and the affinity for binding site do not change by administered drugs. As mGlu₄ PAM binding site may be changed by the drugs due to its characteristic of an allosteric modulator, further evaluation with different types of mGlu₄ PAM drugs

would be helpful to characterize more the radioligand. We did not test blocking compounds other than PXT002331 in this study because the selectivity of the radioligand to mGlu₄ was reported in the previous publication [11]. The radioligand does not have agonist and antagonist activities toward mGlu₁, mGlu₂, mGlu₅, and mGlu₆. It has only weak agonist activity on mGlu₈.

SUV values at the peak under the blocking condition were higher than those at the baseline condition (Fig. 1), which may be related to the peripheral blocking of the target by PXT002331 or the anesthesia effect of induction of ketamine and maintenance of sevoflurane [23]. The visual inspection of the TACs was not sufficient to evaluate the blocking effect because there is no reference region for the mGlu₄ receptor. Therefore, the quantitative analysis with arterial input function was made to evaluate the blocking effects.

Whole-body PET showed high accumulation of [¹¹C]PXT012253 in the liver, kidney, heart, and brain in the initial phase. The radioligand was excreted through both the gastrointestinal and the urinary tracts. The effective dose of [¹¹C]PXT012253 was 0.0042 mSv/MBq, which is just below the median of other reported C11-labeled PET radioligands (0.0047 mSv/MBq) [24]. It suggested that 3–4 times PET measurements using approximately 300 MBq of [¹¹C]PXT012253 per PET measurement for the same subjects can be performed within 5 mSv in total radiation exposure in the further clinical PET study.

In this study, unintentionally, the brain PET scans were performed in male NHPs while whole-body scans were performed in female NHPs. The limitation was the blood volume to take from NHPs during PET scans in 1 day that is determined based on the NHPs' body weight. Therefore, larger NHPs tend to be used for PET scans with arterial samples. For the whole-body PET scans, relatively smaller NHPs tend to be used because there are only few blood samples if there are and the smaller body size help to scan the whole body with fewer bed positions. As the body weights of male NHPs are in general heavier than those of female NHPs among the NHPs we used, the current proportion of female and male NHPs occurred with no intention. Thus, the current data set does not allow a direct assessment of gender effect, for example, on a potential difference between female and male NHPs in the metabolism of the radioligand in the whole body.

Conclusions

[¹¹C]PXT012253 is a promising PET radioligand for mGlu₄ allosteric modulators in the brain. MA1 would be the choice of quantitative method for [¹¹C]PXT012253. Based on the dosimetry results, multiple PET measurements in the same subjects can be performed, which is useful for the target occupancy or longitudinal studies. Further development of [¹¹C]PXT012253 in human subjects is warranted.

Acknowledgements. We thank all members of the Karolinska Institutet PET Centre for assistance with the PET experiments.

Compliance with Ethical Standards. The study was approved by the Animal Ethics Committee of the Swedish Animal Welfare Agency and was performed according to “Guidelines for planning, conducting and documenting experimental research” (Dnr 4820/06-600) of Karolinska Institutet.

Conflict of Interest

This work was sponsored by Prexton Therapeutics. Delphine Charvin and Guillaume Duvey are employees of Prexton Therapeutics. All other authors declare that they have no conflict of interest.

References

- Zanotti-Fregonara P, Xu R, Zoghbi SS, Liow JS, Fujita M, Veronese M, Gladding RL, Rallis-Frutos D, Hong J, Pike VW, Innis RB (2016) The PET radioligand 18F-FIMX images and quantifies metabotropic glutamate receptor 1 in proportion to the regional density of its gene transcript in human brain. *J Nucl Med* 57:242–247
- Wong DF, Waterhouse R, Kuwabara H, Kim J, Brasic JR, Chamroonrat W, Stabins M, Holt DP, Dannals RF, Hamill TG, Mozley PD (2013) ¹⁸F-FPEB, a PET radiopharmaceutical for quantifying metabotropic glutamate 5 receptors: a first-in-human study of radiochemical safety, biokinetics, and radiation dosimetry. *J Nucl Med* 54:388–396
- Kimura Y, Siméon FG, Zoghbi SS, Zhang Y, Hatazawa J, Pike VW, Innis RB, Fujita M (2012) Quantification of metabotropic glutamate subtype 5 receptors in the brain by an equilibrium method using ¹⁸F-SP203. *Neuroimage* 59:2124–2130
- Lohith TG, Tsujikawa T, Siméon FG, Veronese M, Zoghbi SS, Lyoo CH, Kimura Y, Morse CL, Pike VW, Fujita M, Innis RB (2017) Comparison of two PET radioligands, [¹¹C]FPEB and [¹¹C]SP203, for quantification of metabotropic glutamate receptor 5 in human brain. *J Cereb Blood Flow Metab* 37:2458–2470
- Esterlis I, DellaGioia N, Pietrzak RH et al (2017) Ketamine-induced reduction in mGluR5 availability is associated with an antidepressant response: an [¹¹C]ABP688 and PET imaging study in depression. *Mol Psychiatry* 23:824–832
- DeLorenzo C, Gallezot JD, Gardus J, Yang J, Planeta B, Nabulsi N, Ogden RT, Labaree DC, Huang YH, Mann JJ, Gasparini F, Lin X, Javitch JA, Parsey RV, Carson RE, Esterlis I (2017) *In vivo* variation in same-day estimates of metabotropic glutamate receptor subtype 5 binding using [¹¹C]ABP688 and [¹⁸F]FPEB. *J Cereb Blood Flow Metab* 37:2716–2727
- Charvin D (2018) mGlu₄ allosteric modulation for treating Parkinson’s disease. *Neuropharmacology* 135:308–315
- Sebastianutto I, Cenci MA (2018) mGlu receptors in the treatment of Parkinson’s disease and L-DOPA-induced dyskinesia. *Curr Opin Pharmacol* 38:81–89
- Marino MJ, Williams DL Jr, O’Brien JA et al (2003) Allosteric modulation of group III metabotropic glutamate receptor 4: a potential approach to Parkinson’s disease treatment. *Proc Natl Acad Sci U S A* 100:13668–13673
- Charvin D, Di Paolo T, Bezard E, et al. (2018) A mGluR4 positive allosteric modulator alleviates parkinsonism in primates. in press
- Kil KE, Poutiainen P, Zhang Z, Zhu A, Kuruppu D, Prabhakar S, Choi JK, Tannous BA, Brownell AL (2016) Synthesis and evaluation of N-(methylthiophenyl)picolinamide derivatives as PET radioligands for metabotropic glutamate receptor subtype 4. *Bioorg Med Chem Lett* 26:133–139
- Kil K, Zhang Z, Zhu A et al (2014) Radiosyntheses and preclinical evaluation of two N-(3-[¹¹C]methylthiophenyl)-2-picolinamide ([¹¹C]ML128) derivatives as radiotracers for mGlu₄. *J Nucl Med* 55(supplement 1):1169
- Andersson J, Truong P, Halldin C (2009) In-target produced [¹¹C]methane: increased specific radioactivity. *Appl Radiat Isot* 67:106–110
- Varrone A, Sjöholm N, Eriksson L, Gulyás B, Halldin C, Farde L (2009) Advancement in PET quantification using 3D-OP-OSEM point spread function reconstruction with the HRRT. *Eur J Nucl Med Mol Imaging* 36:1639–1650
- Logan J, Fowler JS, Volkow ND, Wolf AP, Dewey SL, Schlyer DJ, MacGregor RR, Hitzemann R, Bendriem B, Gatley SJ, Christian DR (1990) Graphical analysis of reversible radioligand binding from time-activity measurements applied to [N-11C-methyl]-(-)-cocaine PET studies in human subjects. *J Cereb Blood Flow Metab* 10:740–747
- Ichise M, Toyama H, Innis RB, Carson RE (2002) Strategies to improve neuroreceptor parameter estimation by linear regression analysis. *J Cereb Blood Flow Metab* 22:1271–1281
- Akaike H (1976) An information criterion (AIC). *Math Sci* 14:5–9
- Lassen NA, Bartenstein PA, Lammertsma AA, Prevett MC, Turton DR, Luthra SK, Osman S, Bloomfield PM, Jones T, Patsalos PN, O’Connell MT, Duncan JS, Andersen JV (1995) Benzodiazepine receptor quantification *in vivo* in humans using [¹¹C]flumazenil and PET: application of the steady-state principle. *J Cereb Blood Flow Metab* 15:152–165
- Stabin MG, Sparks RB, Crowe E (2005) OLINDA/EXM: the second-generation personal computer software for internal dose assessment in nuclear medicine. *J Nucl Med* 46:1023–1027
- Makoff A, Lelchuk R, Oser M, Harrington K, Emson P (1996) Molecular characterization and localization of human metabotropic glutamate receptor type 4. *Brain Res Mol Brain Res* 37:239–248
- Kil KE, Poutiainen P, Zhang Z, Zhu A, Choi JK, Jokivarsi K, Brownell AL (2014) Radiosynthesis and evaluation of an ¹⁸F-labeled positron emission tomography (PET) radioligand for metabotropic glutamate receptor subtype 4 (mGlu₄). *J Med Chem* 57:9130–9138
- Niswender CM, Conn PJ (2010) Metabotropic glutamate receptors: physiology, pharmacology, and disease. *Annu Rev Pharmacol Toxicol* 50:295–322
- Arakawa R, Farde L, Matsumoto J, Kanegawa N, Yakushev I, Yang KC, Takano A (2018) Potential effect of prolonged sevoflurane anesthesia on the kinetics of [¹¹C]raclopride in non-human primates. *Mol Imaging Biol* 20:183–187
- Zanotti-Fregonara P, Innis RB (2012) Suggested pathway to assess radiation safety of ¹¹C-labeled PET tracers for first-in-human studies. *Eur J Nucl Med Mol Imaging* 39:544–547